Solar-blind ultraviolet band-pass filter based on metal–dielectric multilayer structures*

Wang Tian-Jiao(王天娇), Xu Wei-Zong(徐尉宗), Lu Hai(陆 海)†, Ren Fang-Fang(任芳芳), Chen Dun-Jun(陈敦军), Zhang Rong(张 荣), and Zheng You-Dou(郑有炓)

Key Laboratory of Advanced Photonic and Electronic Materials of Jiangsu Province, and School of Electronic Science and Engineering, Nanjing University, Nanjing 210093, *China*

(Received 28 October 2013; revised manuscript received 29 November 2013; published online 29 May 2014)

Solar-blind ultraviolet (UV) band-pass filter has significant value in many scientific, commercial, and military applications, in which the detection of weak UV signal against a strong background of solar radiation is required. In this work, a solar-blind filter is designed based on the concept of "transparent metal". The filter consisting of Al/SiO_2 multilayers could exhibit a high transmission in the solar-blind wavelength region and a wide stopband extending from near-ultraviolet to infrared wavelength range. The central wavelength, bandwidth, Q factor, and rejection ratio of the passband are numerically studied as a function of individual layer thickness and multilayer period.

Keywords: solar-blind band-pass filter, metal–dielectric multilayer

PACS: 42.25.Bs, 78.20.–e, 78.20.Bh, 85.60.Gz **DOI:** 10.1088/1674-1056/23/7/074201

1. Introduction

The detection of optical radiation in the deep ultraviolet (UV) wavelength range has drawn increasing attention due to many key applications, such as missile plume detection, flame warning, chemical/biological sensing, pollution monitoring, and solar astronomy.[1,2] Although wide-bandgap semiconductors, such as AlGaN and SiC, are believed to be the promising candidate materials for the fabrication of UV photodetectors (PDs), high material cost and immature device processing techniques hinder the wide applications of those PDs, which are still in early development stage.[3–5] Meanwhile, considering currently available mature and cheap silicon processing technologies, UV PDs based on silicon would greatly benefit from potentially low cost and easiness for large-scale integration. However, Si-based PDs also have strong photo-response to visible and near-infrared radiation, which in standard conditions often exceeds the UV signal to be detected by three to four orders of magnitude and could completely mask the useful signal.[6] Therefore, to selectively detect UV radiation, Si-based PDs have to integrate with a UV band-pass filter that strongly rejects unwanted visible and infrared background radiation.

All-dielectric filters based on alternative dielectric stacks with low and high refractive indices have been employed to obtain a UV band-pass filter.[7] However, due to the interference nature of the dielectric filter, the filter structure presents a periodic transmission property, which means that a passband in deep UV range is always accompanied by unwanted passbands in visible and infrared wavelength range. To suppress the parasitic passbands, additional dielectric stacks with different optical parameters must be added in the filter design, which in turn increases fabrication complexity and cost. Thus, in spite of their relatively high transmission coefficient in the desired passband, all-dielectric filters have restricted applications for Si-based UV PDs.

Another applicable design of UV bandpass filters is based on metal/dielectric multilayers, in which utilized is a metal layer with the strong capability for blocking visible and infrared radiation. More specifically, if a metal–dielectric–metal Fabry–Pérot cavity structure is adopted in the filter design, the filter could exhibit a unique feature: transmitting short wavelength light at resonant frequencies, while presenting a huge stop band at longer wavelengths. This so-called "transparent metal theory" has been described in several previous studies.[8] Some band-pass filter for near-UV (300–400 nm) or visible wavelength range have been designed and implemented.[9–11]

In this work, given the importance of selectively detecting deep UV signal, a solar-blind (240–280 nm) band-pass filter is firstly designed based on the concept of "transparent metal theory". A simple and general, yet efficient approach is presented in filter design, which is illustrated by Al/SiO_2 thin film stacks deposited on a sapphire substrate. High-performance solar-blind filter is obtained through design optimization, and the tradeoffs between filter bandwidth and peak transmission are discussed.

*Project supported by the National Basic Research Program of China (Grant Nos. 2010CB327504, 2011CB922100, and 2011CB301900), the National Natural Science Foundation of China (Grant Nos. 60936004 and 11104130), the Natural Science Foundation of Jiangsu Province, China (Grant Nos. BK2011556 and BK2011050), and the Priority Academic Program Development of Jiangsu Higher Education Institutions, China.

†Corresponding author. E-mail: hailu@nju.edu.cn

© 2014 Chinese Physical Society and IOP Publishing Ltd

2. Analysis method

In this work, besides analytical approach, the detailed transmission spectrum of the filter under design is calculated using transfer matrix method,[12–14] in which, based on the continuity conditions of electromagnetic field, the system transfer matrix is used to determine the reflection and transmission coefficients of light passing through a multilayer structure. Specifically, considering a multilayer structure composed of $N+1$ layers with complex refractive indices and N interfaces (see Fig. 1), the field amplitudes in each layer can be calculated by a product of 2×2 matrices in sequence as shown in the following equation:[12]

$$\begin{pmatrix} F_{m-1} \\ B_{m-1} \end{pmatrix} = \underbrace{\begin{pmatrix} \mathrm{e}^{-\mathrm{i}\delta_{m-1}} & 0 \\ 0 & \mathrm{e}^{\mathrm{i}\delta_{m-1}} \end{pmatrix}}_{P_{m-1}} \times \underbrace{\frac{1}{t_{m-1}} \begin{pmatrix} 1 & r_{m-1,m} \\ r_{m-1,m} & 1 \end{pmatrix}}_{R_{m-1}} \begin{pmatrix} F_m \\ B_m \end{pmatrix}, \quad (1)$$

where F and B represent the amplitudes of forward and backward waves respectively, and their subscripts indicate the specific layer of medium through which the light is passing.

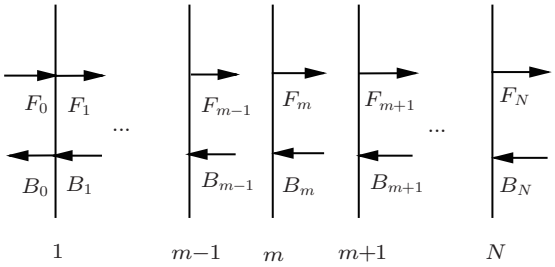


Fig. 1. Notation of field amplitudes within an arbitrary multilayer structure.

Moreover, in Eq. (1) the bulk effect of each layer is represented by its propagation matrix $\boldsymbol{P}$, and the interface effect is presented by the refraction matrix $\boldsymbol{R}$. In addition, $\delta_{m-1} = 2\pi k n_{m-1} d_{m-1}$ is the phase thickness imposed by the bulk of the $(m-1)$ layer upon one traversal of light. Here k is the wave number, n_{m-1} and d_{m-1} are the refractive index and the thickness of each layer, respectively. The system transfer matrix can be reduced to[12]

$$\begin{pmatrix} F_0 \\ B_0 \end{pmatrix} = R_{0,1}^{-1} \left[\prod_{m=1}^{N-1} P_m R_{m,m+1} \right] \begin{pmatrix} F_N \\ B_N \end{pmatrix} = \begin{pmatrix} T_{11} & T_{12} \\ T_{21} & T_{22} \end{pmatrix} \begin{pmatrix} F_N & B_N \end{pmatrix}. \quad (2)$$

Thus, the net reflection coefficient of a multilayer structure can be calculated as $r_{0,N} = B_0/F_0|_{B_{N=0}} = T_{21}/T_{11}$, and the corresponding net transmission coefficient $t_{0,N} = F_N/F_0|_{B_{N=0}} = 1/T_{11}$.

In this work, a solar-blind filter based on Al/SiO_2 multilayers grown on a sapphire substrate is designed as an example. Silica and sapphire are both highly transparent in UV region and their refractive indices are 1.57 and 1.8 respectively in a wavelength range of interest.[15] Al is chosen due to its relatively low plasma frequency (corresponding plasma wavelength is ∼ 83 nm). Experimental data for the optical constants of Al are adopted from the work of Rakić[16] and are fitted in a wavelength range of interest from 100 nm to 700 nm. The real part of the Al refractive index is found as

$$N_{\mathrm{Al}}(\lambda) = a_1 \lambda^{b_1},$$

where $a_1 = 4.366$ and $b_1 = 2.396$. The extinction coefficient of Al can be expressed as

$$K_{\mathrm{Al}}(\lambda) = a_2 \lambda + b_2,$$

where $a_2 = 12.52$ and $b_2 = -0.2956$. The original experimental curves and the fitted data points are shown in Fig. 2.

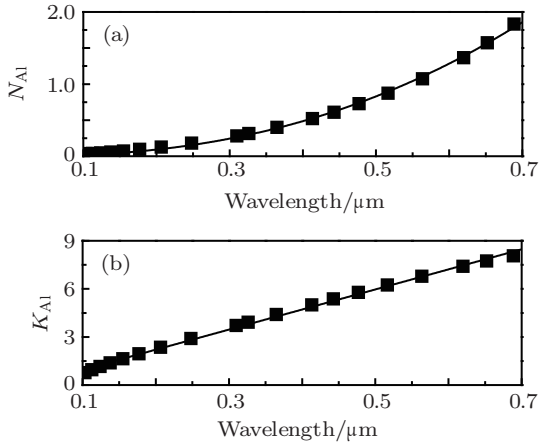


Fig. 2. (a) Fitted refractive index N_{Al} and (b) extinction coefficient K_{Al} of aluminum versus wavelength.

3. Structure design

3.1. Transparent metal theory

Light with wavelength above the plasma wavelength (83 nm for Al) can only propagate a small distance inside a metal before most of it is reflected. This characteristic length is called skin depth (SD) and is defined as the depth at which the intensity of the radiation inside the metal falls to $1/e$-fold of its original value just beneath the surface. The skin depth can be expressed in terms of light frequency ω or wavelength λ, and the imaginary component of the refraction index k as follows: $\mathrm{SD} = c/2k\omega = \lambda/4\pi k$, where c is the speed of light in vacuum.[8] Taking Al for example, when $\lambda = 320$ nm, then $k = 3.7$ (see Fig. 2) and SD is calculated to be ∼7 nm. Furthermore, at longer wavelength, SD would drop off quickly due to the sharper increase in the extinction coefficient k. Therefore, a thin metal film of tens of nm in thickness should be very effective to block incoming light ranging from UV to infrared.

However, if a metal–dielectric–metal periodic structure is employed, the transmission properties could be very different. For example, considering a single 30-nm Al film suspended in air, calculation based on transfer matrix method indicates that the Al film is a good light blocker with a transmission coefficient of below 5% in the wavelength range of interest (dashed line in Fig. 2). On the other hand, if the original 30 nm film is sliced into two 15 nm films with a spacing of 100 nm in air, as shown by the lower inset of Fig. 3, the transmission coefficient of the structure then increases to 80% at 130 nm and 40% at 260 nm, respectively (solid line in Fig. 3).

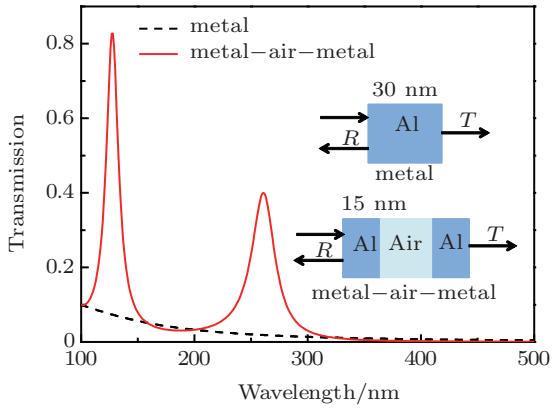


Fig. 3. (color online) Transmission spectra of a metal–air–metal sandwich structure (solid line) and a solid metal film (dash line). Insets show schematics of the two structures respectively.

The different transmission properties can be explained as follows: the structure consisting of two metal films spaced by a dielectric layer could form a thin film Fabry–Pérot cavity (or multiple cavities if there are more periods), given the condition that the sandwiched dielectric layer has an appropriate thickness. Since the Fabry–Pérot cavity has two opposite mirror-like interfaces, the incident light confined within the cavity would reflect back and forth many times. For a fixed cavity length, the reflected light and initial light would be in phase (constructive interference) at certain wavelengths, leading to an enhanced light intensity within the cavity and then higher net transmission rate at the resonant wavelengths.[8] Meanwhile, due to the high extinction coefficient k of metal at longer wavelength, overall transmission and possible resonant peaks in visible and infrared wavelength ranges are effectively suppressed.

3.2. Solar-blind UV filter

The solar-blind filter under design is based on an Al/SiO_2/Al sandwich structure grown on a sapphire substrate. According to the optical resonance theory, the transmission spectrum curve would peak at λ when the following condition is met:

$$\Phi_{\mathrm{DM1}} + \Phi_{\mathrm{DM2}} + \frac{2\pi}{\lambda} 2nD = 2m\pi, \tag{3}$$

where Φ_{DM1} and Φ_{DM2} are the phase changes of reflection $R(\lambda)$ at interface 1 and interface 2 respectively as shown in the inset of Fig. 4. The third term on the left-hand side of Eq. (3) is the optical path length of the dielectric back and forth, in which D is the thickness of dielectric layer. In addition, m is the order of resonance and should be larger than or equal to zero. Based on Fresnel equation, under normal incidence condition, $R(\lambda) = (n_{\mathrm{D}} - n_{\mathrm{E}})/(n_{\mathrm{D}} + n_{\mathrm{E}})$, where n_{D} is the refractive index of the dielectric layer, and n_{E} is the equivalent complex refractive index of the metal layer and the outside layer. Here the outside layer is air for interface 1 or sapphire for interface 2. Since the complex refractive index of Al is a strong function of wavelength λ, n_{E} and Φ_{DM} are both sensitive functions of metal thickness and wavelength as well.

To design a solar-blind UV filter with passband centered at 260 nm and a wide stop band ranging from 280 nm to near infrared, the thickness of each Al layer is first assumed to be 15 nm. At $\lambda = 260$ nm, R_1 and R_2 are determined to be $-0.371 - 0.734\mathrm{i}$ and $-0.414 - 0.678\mathrm{i}$, respectively. The sum of Φ_{DM1} and Φ_{DM2} is then calculated to be -1.349π. Based on Eq. (3), when $m = 0$, the thickness of the inner SiO_2 layer is determined to be $D = 55.845$ nm (55 nm is chosen for simulation). Finally, transfer matrix method is used to calculate the detailed transmission spectrum numerically. As shown in Fig. 4, a solar-blind filter is realized through the above design with a peak transmission of 47% at 260 nm and a full-width-at-half-maximum (FWHM) of 38 nm for the UV passband. When wavelength is longer than 300 nm, the transmission of the filter is below 5%.

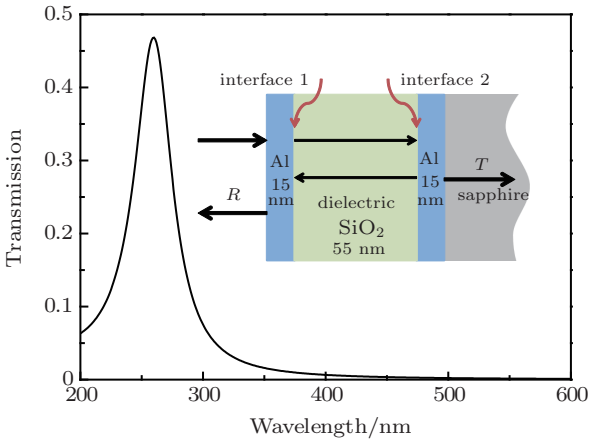


Fig. 4. (color online) Transmission spectrum of the Al/SiO_2/Al/sapphire solar-blind filter. Inset shows the schematic of the filter structure.

3.3. Parameter optimization

3.3.1. Thickness of the dielectric layer

The effect of dielectric layer thickness on transmission properties is studied for the Al/SiO_2/Al/sapphire filter structure. Here the thickness values of two Al layers are both fixed at 15 nm for easy comparison. As shown in Fig. 5, the peak

transmission wavelength of the bandpass filter is tunable from 210 to 310 nm, when the thickness of the dielectric layer increases from 40 to 70 nm. Meanwhile, the overall transmission of the filter drops off by $\sim 27\%$. The above simulation results can be understood based on Eq. (3). Since thicker dielectric layer means longer optical path, a longer wavelength is required to meet the resonance condition. Besides, if the dielectric layer is even thicker, m may be 1, 2, 3, or larger to fit the equation, which means higher order of resonant peaks might appear in UV range (not shown). The overall transmission drop of the passband should be caused by the enhanced optical blocking capability of the metal film at longer wavelength. As has been discussed in the above section, the skin depth of metal film decreases as wavelength increases.

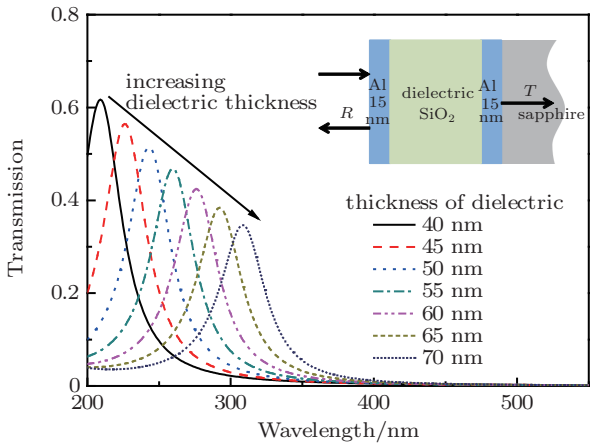


Fig. 5. (color online) Transmission spectra of the Al/SiO_2/Al/sapphire multilayer structure at different values of SiO_2 thickness. Inset shows the schematic of the filter structure.

3.3.2. Thickness of the metal layer

The effect of metal layer thickness on the performance of the solar-blind filter is also studied. Here the thickness of dielectric layer is fixed at 55 nm, corresponding to zero order resonance condition. As shown in Fig. 6, a tradeoff between FWHM and peak transmission of the passband can be observed. Specifically, when the thickness of the Al layer increases from 8 to 18 nm, the FWHM of the passband narrows from 116 to 27 nm, while the peak transmission drops off from 69% to 37%. Besides, the peak wavelength of the passband slightly shifts from 272 nm to 257 nm.

The drop of peak transmission can be easily explained by the enhanced light blocking capability of thicker metal film. The variation of FWHM can be understood based on the Q factor of the metal Fabry–Pérot cavity. In resonant cavity theory, the Q factor is a parameter that characterizes a resonator bandwidth relative to its central frequency, namely, $Q = f_0/\Delta f$, where f_0 is the central frequency, and Δf is the bandwidth. In the present case, as the Al layer thickness varies from 8 to 18 nm, Q factor shows a large increase from 2.1 to 9.5. In physics, a higher Q factor means a lower rate of energy loss relative to the stored energy of the resonator. For a metal resonant cavity, the energy loss should be the transmission loss at interface between the inner dielectric and the outside metal medium. For thicker metal layer, the interface reflectance should approach 1, which means smaller energy loss of the resonant cavity. Thus, assuming that the stored energy remains almost unchanged within the cavity, the Q factor would present an increasing tendency, leading to a reduced FWHM. In addition, the small down-shift of peak wavelength of the passband at larger Al film thickness should be caused by the small variations of Φ_{DM} and n_{E} (see Eq. (3)), which are both functions of metal thickness.

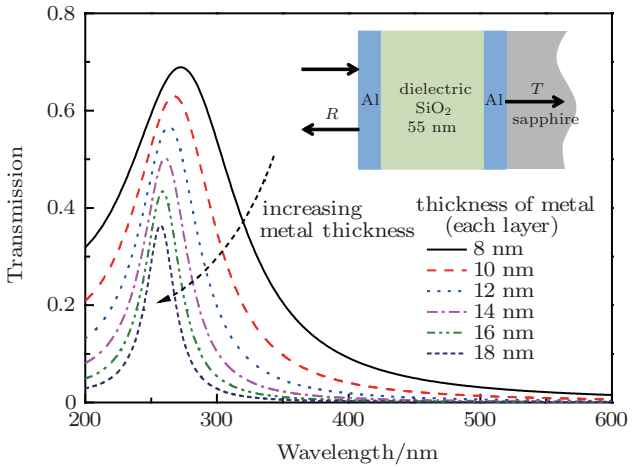


Fig. 6. (color online) Transmission spectra of the Al/SiO_2/Al/sapphire multilayer structure at different values of Al thickness. Inset shows the schematic of the filter structure.

3.3.3. Number of periods

Besides peak wavelength position and FWHM of the passband, rejection ratio is another key performance parameter of an optical bandpass filter, which, in the present case, can be enhanced by adding more periods of the resonant cavity. Here, the rejection ratio R is defined as the ratio of the peak transmission power in passband over the suppressed transmission power in stop band. The transmission properties of the metal–dielectric multilayer filter with different periods are shown in Fig. 7 in semi-log scale. It is found that as the number of periods increases, the width of the passband narrows while an apparent decrease of transmission in the stop band is observed, leading to an enhanced rejection ratio. For instance, when the period number is 5, the rejection ratio calculated as the transmission measured at 260 nm divided by the transmission measured at 400 nm is more than 10^5, while the peak transmission only drops to 0.32. Thus, by optimizing the period number of the metal–dielectric multilayer structure, a high performance solar-blind filter with acceptable peak transmission in the passband and sufficient suppression in visible and near-infrared wavelength ranges can be achieved.

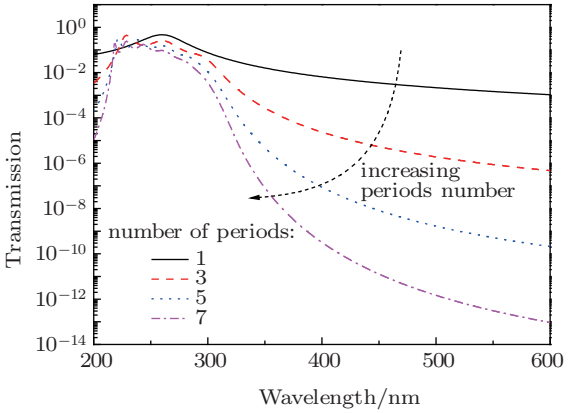


Fig. 7. (color online) Transmission spectra of the $(Al/SiO_2)^p/Al/sapphire$ multilayer filter in semi-log plot, in which p is the period number of the repeating bi-layer structure. Here the thickness values of each Al layer and SiO_2 layer are 15 nm and 50 nm, respectively.

4. Conclusions

Solar-blind filters, each consisting of a metal–dielectric multilayer structure, are numerically designed based on the concept of "transparent metal", in which high transmission can be obtained at desired wavelength if a resonant cavity is properly formed. Meanwhile, sufficient suppressions of stop band in visible and infrared wavelength ranges are realized due to the high extinction coefficient of metal film. The detailed transmission properties of the solar-blind filters are calculated by using a transfer matrix method. The influence of key design parameters on filter performance is discussed. This study suggests that the "transparent metal" concept can be extended to deep UV wavelength region and is applicable for high-performance solar-blind bandpass filters.

References

[1] Razeghi M and Rogalsky A 1996 *J. Appl. Phys.* **79** 7433
[2] Popovic R S 1993 *The 2nd Serbian Conference on Microelectronics and Optoelectronics*, October 26–28, 1993 Nis, Yugoslavia, p. 239
[3] Chen X P, Zhu L H, Cai J and Wu Z Y 2007 *J. Appl. Phys.* **102** 2
[4] Muñoz E, Monroy E, Pau J L, Calle F, Omnès F and Gibart P 2001 *Phys.: Condens. Matter* **13** 7115
[5] Lian H F, Wang G S, Lu H, Ren F F, Chen D J, Zhang R and Zheng Y D 2013 *Chin. Phys. Lett.* **30** 017302
[6] Djurić Z G, Danković T, Jakšić Z S, Randjelović D, Petrović R, Ehrfeld W, Schmidt A and Hecker K 1999 *Proc. SPIE: Design, Test and Microfabrication of MEMS and MOEMS*, March 10, 1999 Paris, France, p. 3680
[7] Celanovic I, O'Sullivan F, Ilak M, Kassakian J and Perreault D 2004 *Opt. Lett.* **29** 863
[8] Scalora M, Bloemer M J, Manka A S, Pethel S D, Dowling J P and Bowden C M 1998 *J. Appl. Phys.* **83** 2377
[9] Bloemer M J and Scalora M 1998 *Appl. Phys. Lett.* **72** 1676
[10] Jakšić Z, Maksimović M and Sarajlić M 2005 *J. Opt. A: Pure Appl. Opt.* **7** 51
[11] Mu J W, Lin P T, Zhang L, Michel J, Kimerling L C, Jaworski F and Agarwal A 2013 *Appl. Phys. Lett.* **102** 213105
[12] Katsdis C C and Siapkas 2002 *Appl. Opt.* **41** 3978
[13] Li Z X, Pei L, Chen H, Peng W J, Ning T G, Zhao R F and Gao S 2010 *Acta Phys. Sin.* **54** 2226 (in Chinese)
[14] Xu T, Cao Z Q and Fang J H 2010 *Chin. Phys. B* **19** 040307
[15] Rakić A D 1995 *Appl. Opt.* **34** 4755
[16] Palik E D 1985 *Handbook of Optical Constants of Solids* (New York: Academic)